Interference Mitigation for Faster-Than-Nyquist *m*CAP in Bandlimited VLC Using Variable GIM Scheme

Yungui Nie
School of Electronic and Information Engineering
Soochow University
Suzhou, China
20234028002@stu.suda.edu.cn

Chen Chen
School of Microelectronics and Communication Engineering
Chongqing University
Chongqing, China
c.chen@cqu.edu.cn

Siming Mo
Jiangsu Etern Co., Ltd
Suzhou, China
msm@yongding.com.cn

Xiaodi You
School of Electronic and Information Engineering
Soochow University
Suzhou, China
xdyou@suda.edu.cn

Qinghai Lu
Jiangsu Etern Co., Ltd
Suzhou, China
luqinghai@yongding.com.cn

Zhihong Zeng
School of Microelectronics and Communication Engineering
Chongqing University
Chongqing, China
zhihong.zeng@cqu.edu.cn

Jinsheng Zhang
Jiangsu Etern Co., Ltd
Suzhou, China
zhangjinsheng@etern-laser.com

*Gangxiang Shen
School of Electronic and Information Engineering
Soochow University
Suzhou, China
shengx@suda.edu.cn

Abstract—A novel variable gapped index modulation (VGIM) scheme is proposed to mitigate the IBI in FTN-*m*CAP for bandlimited VLC systems. Experimental results show that FTN-8CAP-VGIM achieves a substantial SE improvement of 108% compared with 8CAP.

Keywords—visible light communication, faster-than-Nyquist, index modulation, spectral efficiency

I. INTRODUCTION

Visible light communication (VLC) is a wireless communication technology that utilizes light signals in the visible spectrum (400-700 THz) for data transmission, helping to address the shortage of spectrum resources in radio frequency (RF) communication [1]. Although VLC offers significant advantages in terms of spectrum resources, and security, its data rate is constrained by the limited modulation bandwidth of LEDs [2].

To date, several equalization techniques, including pre-equalization [3] and post-equalization [4], have been investigated in VLC systems to extend the available modulation bandwidth. Moreover, various spectrally efficient modulation techniques have been employed in VLC systems to enhance the achievable data rate, such as carrierless amplitude and phase modulation (CAP) [5] and orthogonal frequency division multiplexing (OFDM) [2]. CAP modulation is regarded as a promising alternative because it has a lower peak-to-average-power ratio (PAPR) than OFDM and relies on pulse-shaping filters that are less complex than discrete Fourier trans-form (DFT) and inverse discrete Fourier transform (IDFT) operations. In addition, multi-band CAP (*m*CAP) is a variant of traditional CAP that transforms it into a multi-carrier form by dividing the spectrum into multiple subbands, with each subband executing a separate CAP modulation process [6]. To enhance spectral efficiency (SE), faster-than-Nyquist *m*CAP (FTN-*m*CAP) has garnered much attention from researchers [7]. However, FTN-*m*CAP suffers from inter-band interference (IBI), which may affect system performance and cannot be ignored.

Recently, to address the issue of IBI in FTN-*m*CAP for bandlimited VLC systems, various interference mitigation schemes have been proposed [8][9]. Inspired by traditional IM [10][11], a novel modulation scheme, known as gapped index modulation (GIM), has been proposed to mitigate the IBI in FTN-*m*CAP [12]. Other relevant studies on the interference mitigation employing the GIM scheme have not been studied.

Building on the concept of GIM, a novel variable gapped index modulation aided FTN-*m*CAP (FTN-*m*CAP-VGIM) scheme is proposed to mitigate the IBI in FTN-*m*CAP. Comprehensive simulation and experimental results verify the superiority of the proposed FTN-*m*CAP-VGIM scheme.

II. PRINCIPLE OF FTN-*M*CAP-VGIM

Figs. 1 (a) and (b) illustrate the block diagrams of FTN-*m*CAP-VGIM transmitter and receiver, respectively. For the FTN-*m*CAP-VGIM transmitter, as shown in Fig. 1 (a), the input b bits enter a joint gapped index and constellation mapper to perform the FTN-*m*CAP-VGIM mapping. To be more specific, the number of subbands is denoted as m, which represents the subblock length. Within the subblock, k subbands are activated, where k is a variable parameter. The subband signals to be transmitted are then generated based on the gapped index corresponding to each k value and the M-QAM constellation symbols. Let $K = \{0, 1, \cdots, \lceil m/2 \rceil\}$ represent as the set of activated subbands, where $\lceil \cdot \rceil$ is the ceil operator and $\lceil m/2 \rceil$ is the calculated maximum number of activated subbands for m subbands after using the gapped index. Different k value contains one or more gapped indexes. Here we take $m = 6$ and 8 for example. For $m = 6$, the activated subbands set $K = \{0, 1, 2, 3\}$ corresponds to the gapped indexes of {0}, {1}, {3}, {4}, {6}, {1, 4}, {1, 6}, {1, 3, 6} and {1,4,6}, respectively. For $m = 8$, the activated subbands set $K = \{0, 1, 2, 3, 4\}$ corresponds to the gapped indexes of {0}, {1}, {3}, {5}, {8}, {1,3}, {1, 5}, {1, 8}, {3, 8}, {1, 3, 8}, {1, 5, 8}, {2, 5, 8}, {3, 5, 8} and {1, 3, 5, 8}, respectively.

After the FTN-*m*CAP-VGIM mapping, an upsampling operation is independently performed on each subband. Then, the in-phase and quadrature components are separated and

filtered through the FTN in-phase and quadrature filters, respectively. Moreover, a square-root raised cosine (SRRC) with a roll-off factor of α is used as the pulse shaping filter, where $0 \leqslant \alpha \leqslant 1$. The larger the roll-off factor α, the more interference it can resist. The roll-off factor α is set to 0.5. The impulse responses of the FTN in-phase and quadrature filters corresponding to the i-th (i = 1, 2, ⋯, m) subband are expressed as follows

$$f_i^{\mathrm{I}}(t) = g(t)\cos(2\pi f_{c,i} t) \tag{1}$$

$$f_i^{\mathrm{Q}}(t) = g(t)\sin(2\pi f_{c,i} t) \tag{2}$$

where $g(t)$ is the impulse response of the SRRC, and $f_{c,i}$ is the center frequency of the i-th subband, which determines the overlap between subbands and can be written as

$$f_{c,i} = \frac{B}{2m} - \frac{(i-1)\left[\frac{B}{m} + B(\beta - 1)\right]}{m-1} \tag{3}$$

where B represents the total uncompressed bandwidth and is set to 25 MHz, and β ($0 \leqslant \beta \leqslant 1$) represents the spectrum compression factor. When $\beta = 0$, there is no overlap between subbands, which corresponds to the traditional mCAP scheme. The bandwidth after spectrum compression is represented by B', satisfying $\beta = (B\text{-}B')/B$. Subsequently, the in-phase and quadrature output signals are subtracted to generate the signals for the m subbands. Finally, the signals from m subbands are combined to produce the FTN-mCAP-VGIM transmitted signal.

For the FTN-mCAP-VGIM receiver, as shown in Fig. 1 (b), the received signal passes through m pairs of matched filters to extract the real and imaginary components of m subbands. Then, the received signal of each subband undergoes downsampling followed by subband frequency-domain equalization (FDE). Finally, after performing joint gapped index and constellation de-mapping, the output bits are obtained.

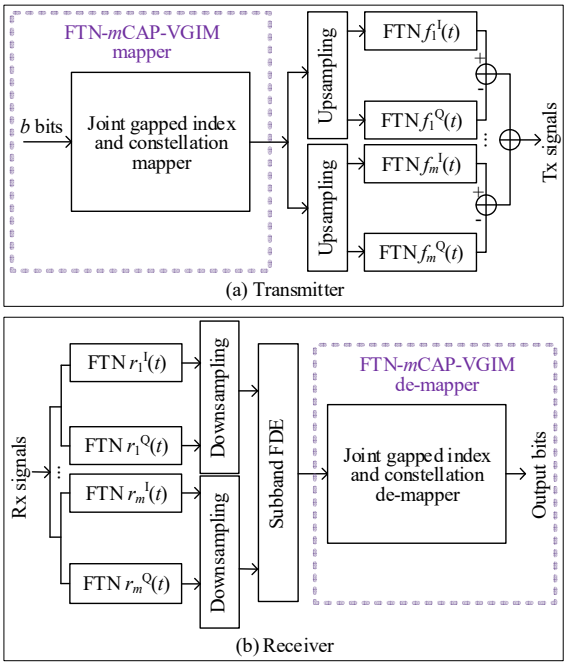

Fig. 1. Block diagram of the proposed FTN-mCAP-VGIM: (a) transmitter and (b) receiver.

Hence, for the proposed FTN-mCAP-VGIM, the input b bits are denoted by

$$b = \left\lfloor \log_2 \left(\sum_{i=0}^{\left\lceil \frac{m}{2} \right\rceil} n_i M^{k_i} \right) \right\rfloor \tag{4}$$

where n_i denotes the gapped index number corresponding to the activated k_i subbands, and $\lfloor \cdot \rfloor$ denotes the floor operator. In bandlimited VLC systems, the SE and data rate for FTN-mCAP-VGIM with an M-QAM constellation are respectively expressed as

$$SE = \frac{\left\lfloor \log_2 \left(\sum_{i=0}^{\left\lceil \frac{m}{2} \right\rceil} n_i M^{k_i} \right) \right\rfloor}{(1+\alpha)(1-\beta)m} \tag{5}$$

$$R = \frac{B \left\lfloor \log_2 \left(\sum_{i=0}^{\left\lceil \frac{m}{2} \right\rceil} n_i M^{k_i} \right) \right\rfloor}{(1+\alpha)m} \tag{6}$$

III. Experiment Setup and Results

In this section, hardware experiments are conducted to evaluate the performance of FTN-mCAP-VGIM in practical bandlimited VLC systems.

A. Parameter Setting

In the section, the numbers of subbands m are set to 6 and 8, respectively. For the case of m = 6, FTN-6CAP, FTN-6CAP-GIM with k = 2 and 3, and FTN-6CAP-VGIM all achieve a data rate of 19.4 Mbps. The required M-QAM constellation orders to achieve the data rate are 4/2/2/2/2/2-QAM, 4/4-QAM, 4/4/2-QAM and 4-QAM, respectively. Similarly, for m = 8, FTN-8CAP, FTN-8CAP-GIM with k = 2, 3 and 4, and FTN-8CAP-VGIM all achieve a data rate of 18.8 Mbps, and the corresponding required M-QAM constellation orders are 4/2/2/2/2/2/2/2-QAM, 8/4-QAM, 4/4/2-QAM, 4/4/4/4/2-QAM and 4-QAM, respectively. The required M-QAM constellation orders to achieve these data rates for m = 6 and 8 are summarized in Table I and Table II, respectively.

TABLE I. Require M-QAM Constellation For M = 6

Schemes	*R = 19.4 Mbps*	*R = 27.8 Mbps*
FTN-6CAP	4/2/2/2/2/2-QAM	4/4/4/4/2/2-QAM
FTN-6CAP-GIM (k = 2)	4/4-QAM	16/8-QAM
FTN-6CAP-GIM (k = 3)	4/4/2-QAM	8/8/4-QAM
FTN-6CAP-VGIM	4-QAM	8-QAM

TABLE II. Require M-QAM Constellation For M = 8

Schemes	*R = 18.8 Mbps*	*R = 25 Mbps*
FTN-8CAP	4/2/2/2/2/2/2/2-QAM	4/4/4/4/2/2/2/2-QAM
FTN-8CAP-GIM (k = 2)	8/4-QAM	16/16-QAM
FTN-8CAP-GIM (k = 3)	4/4/2-QAM	8/8/4-QAM
FTN-8CAP-GIM (k = 4)	4/4/4/4/2-QAM	8/8/4/4-QAM

Schemes	*R = 18.8 Mbps*	*R = 25 Mbps*
FTN-8CAP-VGIM	4-QAM	8-QAM

B. Experimental Setup

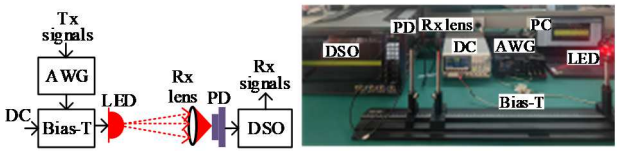

Fig. 2. Experimental setup of an imitation luminous plant red LED-based VLC system. Inset: the measured frequency response of the VLC system.

Fig. 2 shows the experimental setup of a VLC system based on an imitation luminous plant red LED. The digital transmitted signals are initially generated offline using MATLAB, and then loaded into an arbitrary waveform generator (AWG, Rigol DG2102) operating at a sampling rate of 60 MSa/s. The resulting analog signals are superimposed onto a DC bias via a bias-tee (Bias-T, Mini-Circuits ZFBT-6GW+), which are then employed to drive the LED with a wavelength of 660 nm and an optical power of 3 W. After being focused by the Rx lens, the emitted optical signal is detected by a photodetector (PD, Thorlabs PDA10A2). A digital storage oscilloscope (DSO, Rigol DS70504) is used to record the detected signal. Moreover, the photo of the experimental system is shown in the inset of Fig. 2. In addition, the measured frequency response of the VLC system is shown in Fig. 3. The -3 dB bandwidth of the VLC system is about 4 MHz.

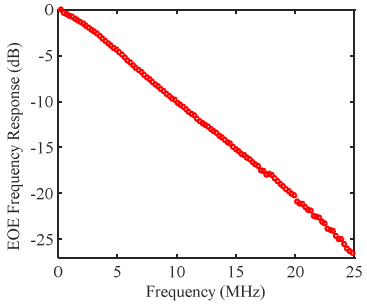

Fig. 3. The measured frequency response of the VLC system.

C. Performance Analysis

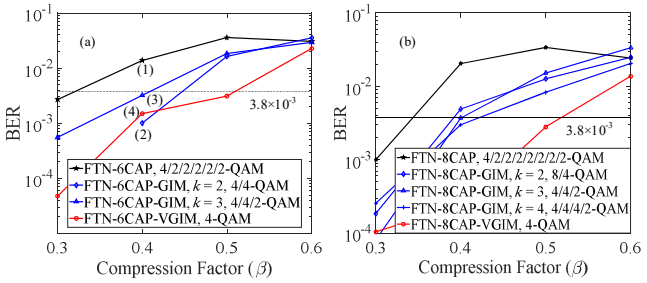

Fig. 4. Experimental BER vs. compression factor for FTN-*m*CAP, FTN-*m*CAP-GIM and FTN-*m*CAP-VGIM with (a) $m = 6$ and (b) $m = 8$.

The experimental BER versus compression factor for FTN-*m*CAP, FTN-*m*CAP-GIM and FTN-*m*CAP-VGIM is shown in Fig. 4, where the transmission distance and the peak-to-peak voltage (Vpp) are respectively set to 50 cm and 2 V. Compared with FTN-*m*CAP and FTN-*m*CAP-GIM, the proposed FTN-*m*CAP-VGIM achieves the largest compression factor under the 7% forward error correction (FEC) coding limit of BER = 3.8×10^{-3}. Specifically, the maximum compression factors achieved by FTN-6CAP-VGIM and FTN-8CAP-VGIM are 0.51 and 0.52, respectively. FTN-8CAP-VGIM obtains the largest bandwidth saving of 13 MHz compared with other schemes. Furthermore, the SE increases from 0.75 bits/s/Hz for 8CAP to 1.56 bits/s/Hz for FTN-8CAP-VGIM with $\beta = 0.52$, corresponding to the SE enhancement of 108%. In addition, the corresponding received spectra of $m = 6$ and $\beta = 0.4$ are depicted in Fig. 5.

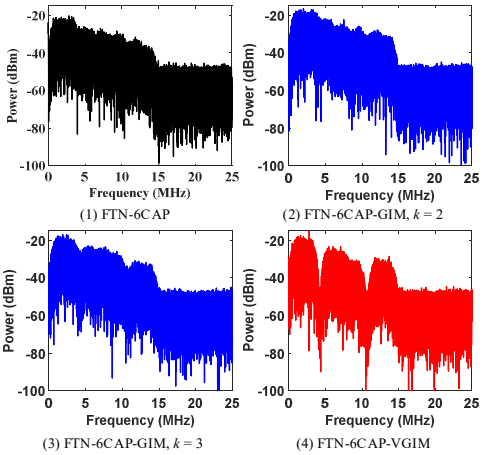

Fig. 5. Received spectrum of different schemes with $m = 6$ and $\beta = 0.4$.

The experimental BER versus Vpp for *m*CAP, FTN-*m*CAP, FTN-*m*CAP-GIM and FTN-*m*CAP-VGIM under different compression factors is shown in Fig. 6. It can be seen that as the Vpp increases, the BER performance of all schemes gradually improves. However, when the compression factor is large, increasing Vpp does not significantly improve BER performance, mainly due to the increase in IBI. For example, when $m = 6$ and $\beta = 0.4$, as shown in Fig. 6 (a), compared with other schemes, to meet the 7% FEC coding limit, the required Vpp of FTN-6CAP-GIM with $k = 2$ is the smallest, which is 0.78 V. When the compression factor increases to 0.45, an Vpp of 1.17 V is required by FTN-6CAP-VGIM, while the required Vpp of 6CAP is 3.20 V.

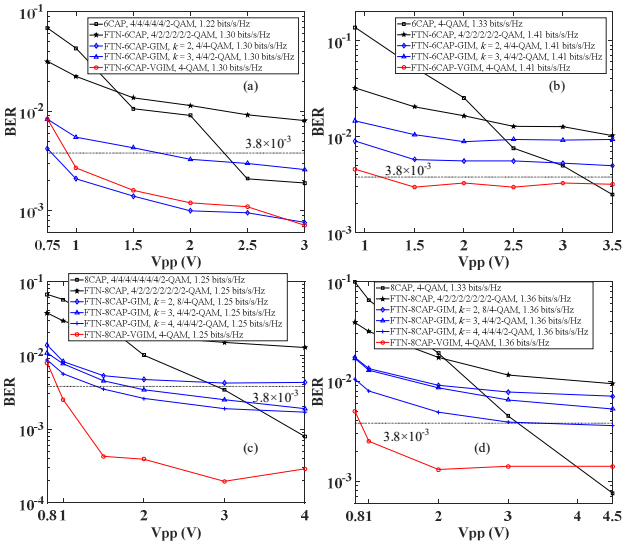

Fig. 6. Experimental BER vs. Vpp for *m*CAP, FTN-*m*CAP, FTN-*m*CAP-GIM and FTN-*m*CAP-VGIM with (a) $m = 6$ and $\beta = 0.4$, (b) $m = 6$ and $\beta = 0.45$, (c) $m = 8$ and $\beta = 0.4$, and (d) $m = 8$ and $\beta = 0.45$.

IV. Conclusion

In this paper, to mitigate the IBI in FTN-*m*CAP, we have proposed and experimentally investigated a novel variable activation subband number scheme, called VGIM, for bandlimited VLC systems. Experimental results show that FTN-8CAP-VGIM supports a maximum compression factor of 0.52, demonstrating a substantial SE improvement of 108% in comparison to 8CAP.

Acknowledgment

This work was supported by the National Nature Science Foundation of China under Grant W2411058, the National Natural Science Foundation of China under Grants 62271091 and 62001319, the Suzhou Science and Technology Bureau-Technical Innovation Project in Key Industries under Grant SYG202112, and the Open Fund of IPOC (BUPT) under Grant IPOC2020A009.

References

[1] N. Chi, Y. Zhou, Y. Wei, and F. Hu, "Visible light communication in 6G: advances, challenges, and prospects," *IEEE Vehicular Technology Magazine*, vol. 15, pp. 93–102, Dec. 2020.

[2] Y. Nie, C. Chen, S. Savovic, Z. Wang, R. Min, X. You, Z. Zeng, and G. Shen, "0.5-bit/s/Hz fine-grained adaptive OFDM modulation for bandlimited underwater VLC," *Optics Express*, vol. 32, pp. 4537-4552, Jan. 2024.

[3] C. Chen et al., "Digital pre-equalization for OFDM-based VLC systems: centralized or distributed?," *IEEE Photonics Technology Letters*, vol. 33, pp. 1081–1084, Aug. 2021.

[4] H. L. Minh et al., "100-Mb/s NRZ visible light communications using a postequalized white LED," *IEEE Photonics Technology Letters*, vol. 21, pp. 1063–1065, May. 2009.

[5] K. O. Akande, P. A. Haigh, and W. O. Popoola, "On the implementation of carrierless amplitude and phase modulation in visible light communication," *IEEE Access*, vol. 6, pp. 60532–60546, Oct. 2018.

[6] M. I. Olmedo et al., "Multiband carrierless amplitude phase modulation for high capacity optical data links," *Journal of Lightwave Technology*, vol. 32, pp. 798–804, Oct. 2014.

[7] J. B. Anderson, F. Rusek, and V. Owal, "Faster-than-Nyquist signaling," *Proceedings of the IEEE*, vol. 101, pp. 1817–1830, Aug. 2013.

[8] W. Niu et al., "Interference mitigation for Faster-Than-Nyquist multiband CAP visible light communication," *Journal of Lightwave Technology*, vol. 42, pp. 1292–1299, Apr. 2024.

[9] P. A. Haigh et al., "Non-orthogonal multi-band CAP for highly spectrally efficient VLC systems," in *International Symposium on Communication Systems, Networks & Digital Signal Processing (CSNDSP)*, 2018, pp. 1-6.

[10] Y. Nie et al., "Multi-mode index modulation aided multi-band CAP with balanced pairwise coding for bandlimited VLC systems," *Journal of Lightwave Technology*, vol. 43, pp. 2053–2066, Mar. 2025.

[11] J. M. Chen et al., "Efficient capacity enhancement using OFDM with interleaved subcarrier number modulation in bandlimited UOWC systems," *Optics Express*, vol. 31, pp. 30723–30734, Sep. 2023.

[12] Y. Nie et al., "Interference mitigation for faster-than-Nyquist *m*CAP in bandlimited VLC: a low-complexity gapped index modulation approach," *Journal of Lightwave Technology*, vol. 43, pp. 6533–6546, Jul. 2025.